

Perturbed voltage-gated channel activity in perturbed bilayers: implications for ectopic arrhythmias arising from damaged membrane

Catherine E Morris¹, Peter F Juranka¹, Béla Joós²

¹OHRI, Ottawa, ON Canada

²Department of Physics, University of Ottawa, Ottawa, ON Canada

Abstract (250 words)

In the ever-beating myocardium, the voltage sensors and pore-gating structures of voltage-gated channels (VGCs) ceaselessly pack and repack. In each VGC, four peripherally-arrayed sensors interact extensively with the sarcolemma's diverse specially-structured bilayers. Their motions, not surprisingly, are mechanosensitive (MS) -- tuned by the bilayer's mechanical state. Structurally-perturbed cardiomyocyte bilayers associated with ischemia, reperfusion, inflammation, cortical-cytoskeleton abnormalities, bilayer-disrupting toxins, diet aberrations, etc, could perturb VGC activity. We characterize VGCs' responses to membranes undergoing bleb-like damage. The facilitation of voltage sensor repacking in these disordered, fluidized bilayers is more accurately "debilitation", since VGCs that activate too easily are "leaky" and could contribute to arrhythmias. Because of differences in sensor-to-gate coupling among different VGCs, their MS leak characteristic fall into two major categories, MS-Speed and MS-Number. A useful way to probe the leak mechanisms is to impose damage (by pipette aspiration of membrane patches), monitoring the irreversible changes until VGCs exhibit exclusively reversible MS responses to stretch. We have characterized Nav1.6 this way, and modeled the consequences (for axons) of MS-Speed-type Nav-leak: mild damage elicits ectopic firing patterns typical of peripheral neuropathies. In mildly-damaged cardiomyocytes, comparable slow- and fast-mode Nav-leak could underlie arrhythmias. Key issues pertaining to MS leak of any specific VGC are: how does bilayer fluidity affect that VGC's rate-limiting voltage-dependent step? what role does VGC mode-switch play in damage-induced activity changes? are reversible/irreversible (elastic/plastic) MS responses comparable? We posit that where pathologically leaky VGCs reside in damaged bilayers, peri-channel bilayer fluidity becomes a critical "target feature" for channel-blocking anti-arrhythmic drugs.

VGC activation is tuned by bilayer structure.

Voltage-gated channels (VGCs) are mechanosensitive (MS) integral membrane proteins [67][55][50]. Their probability of being open (P_{open}) depends primarily on V_m (membrane voltage) but is unavoidably modulated by the variable mechanical states of the bilayers in which they reside. When V_m changes, a VGC's four peripherally-located positively-charged voltage sensors "repack" relative to the channel's central pore region. Repacking sensors pull on "gates". If gates open, ions flow through the central pore [86][31]. The ease and hence speed of voltage sensor repacking depends on structural specifics of the adjacent bilayer lipids, molecules that must, themselves, repack to accommodate voltage sensor repacking. Whether transient or sustained, therefore, perturbations of bilayer structure perturb sensor motions. The mutual rearrangements are easier in highly fluid ("sol-like") bilayers, harder in highly ordered ("gel-like") bilayers. Accordingly, for any VGC in its native setting, activity is tuned by the mechanical state of the lipid matrix.

Before discussing how, for different VGCs, perturbed bilayer/sensor interactions result in two categories of MS modulation -- MS-Speed and MS-Number -- (summarized in **Fig 1**), we illustrate the perils of MS modulated VGC activity in excitable cells with damaged bilayer. The scenario: voltage-gated sodium (Nav) channels triggering ectopic activity in mildly traumatized axons (**Fig 2**). The simulated outcomes robustly show the hallmark features of ectopic neuropathic firing in peripheral neuropathies. Previously, more complicated (and less well-justified biophysically) scenarios involving multiple Nav channel subtypes have been invoked to explain such behaviors. Cardiac arrhythmias originating from peri-infarct zones might similarly be initiated or exacerbated by Nav, Cav, HCN and Kv channels [18][15][48][58][64][21] in mildly-damaged and hence structurally perturbed sarcolemmal bilayer. If this view of dysfunctional excitability in "sick excitable cells" proves correct, then as we have argued in the context of amphiphilic Nav inhibitors and injured axons [52], renewed attention (see [45]) is warranted to the bilayer-partitioning attributes of amphiphilic VGC inhibitors. Ideally, drugs used to block VGCs in sick excitable cells would partition with greater avidity into fluidized, damaged bilayer than into healthy well-packed bilayer.

Ectopic "pacemaking" and leaky Nav channels in damaged membrane. Nav channels can become leaky in many excitable membranes, including Nav-rich myelinated axons [85][73][66] subjected to insult (ischemia, reperfusion injury, inflammatory injury, trauma). "Sick cell Nav-leak" is usually attributed to slow-mode Nav channels but we suggest that fast-mode channels too would contribute [83][8]. With Nav channels distributed at ~1% slow-mode, 99% fast-mode, steady-state fast-mode current (=window current) is the dominant "persistent I_{Na} " at voltages near firing threshold. Then, as V_m depolarizes through the window conductance region, slow-mode I_{Na} would dominate (Fig 4D in [52]). Recombinant Nav1.6 behavior implicates both Nav channels modes in Nav-leak; we found [83][52] that with membrane injury, both slow- and fast-mode Nav channels undergo irreversible hyperpolarizing (left) shifts. If native g_{Na} behaves similarly, both modes will contribute to damage-induced Nav-leak and the fast-mode Nav channels will activate at levels that, in a healthy cell, would be in the subthreshold V_m range [8].

Left-shifted activation curves ($g(V)$) (**Fig 1**, MS-Speed panel; **Fig 2A**) are expected for Nav channels if voltage sensors move too easily in disordered, fluidized bilayers {54}. Cardiomyocytes spend a larger fraction of time depolarized than do axons. Slow-mode g_{Na} would therefore normally contribute more to the persistent Na^+ influxes of cardiomyocytes {58}{48}{39}{84} than in axons. This would be all the more true where g_{Na} became left-shifted in the form of a sick-cell Nav-leak. This idea will need to be addressed experimentally and computationally. To date, what we have modeled regarding slow and fast gating is relatively simple: voltage-clamped membrane with co-existing non-inactivating and fast-inactivating g_{Na} with left-shifted Nav-leak {52}. The aim was simply to assess how sawtooth ramp clamp experiments could be used to help dissect fast/slow g_{Na} -leak sub-components during progressive membrane damage. More accurate models (with kinetically interconnected slow- and fast-inactivating Nav channel states{37}) applied to healthy vs damage-simulated membranes will be needed to guide experimental approaches in cardiomyocyte pathophysiology and pharmacology.

To date, our excitable cell computations on left-shift Nav-leak have been for axons. The particular goal was to assess the impact of the overlooked component – i. e., fast-mode Nav-leak. **Fig 2A** and **Fig 2B** illustrate $I_{Na}(t)$ data from Nav1.6 channels in oocyte membrane patches pre- and post-stretch (stretch imposed by pipette-aspiration). Consistent with such data we devised a biophysically precise, but computationally tractable model of fast-mode based Nav injury. Our Hodgkin-Huxley based injury model is **Nav-CLS**, for “coupled left-shift”. When Nav fast-activation left-shifts, fast-inactivation (a voltage-independent process whose speed is limited by and thence coupled to activation) left-shifts by the same number of millivolts. Note that in Nav-CLS, when m^3 and h (gating parameters) left-shift by a given amount (a large shift, 20 mV, is shown in **Fig 2A top**) the window conductance, $m^3h(V)$, necessarily left-shifts by that amount (**bottom**). Traces in **Fig 2B** are from a membrane whose stretch-induced injury happened to have caused a precisely 20 mV left-shift of $g_{Na}(V)$. An experimental “footnote”: injury intensity becomes evident post-hoc but cannot be precisely controlled while it is being inflicted. For Nav-CLS injury, variable injury intensity corresponds to the plastic zone of MS-Speed in **Fig 1**. As pipette aspiration progressively takes an intact patch to a maximally injured (“saturated”) condition, the value of Nav-CLS (0 mV for intact membranes) can grow to as much as 35 or 40 mV at saturation {75}{83}{6}. Moreover, because of unintended seal formation damage, the intentionally imposed injury might not start from a true Nav-CLS=0 mV. **Fig 2 Bi** shows $I_{Na}(t)$ at -15 mV before and after (pre, post) stretch. Then, from that patch, **Bii** shows that peak-normalized $I_{Na}(t)$ traces overlap perfectly for pre-stretch at x mV, post-stretch at $(x-20)$ mV, as labeled. Thus post-stretch- $I_{Na}(t)$ is kinetically equivalent to intact- $I_{Na}(t)$ 20 mV to the “left. This is a 20 mV Nav-CLS injury.

In Nav-CLS injury, the shifted component of window current from a damaged region of membrane is essentially a pathological “subthreshold persistent I_{Na} ”. In pacemaking interneurons, fast-mode based subthreshold persistent I_{Na} serves as a pacemaker current {77} but for axons pacemaking is anathema and likewise for, say, ventricular cardiomyocytes.

For Nav-CLS injury modeled in axons, we varied both the fraction of total g_{Na} affected and injury intensity {8}. Projecting our axon model findings on ectopic firing, propagation block, and ionic dysregulation to cardiomyocytes suggests that damaged regions of membrane in

those excitable cells could yield similar problems. Cardiac Nav1.6 (dominant isoform in sinoatrial node cells {37}) is certainly of interest, but the possibility of pathologic MS modulation of Nav1.5, the major cardiac isoform would also be worth pursuing. We know **a**) that stretch co-accelerates the (coupled) activation/fast-inactivation time courses of Nav1.5 {54}{4} and **b**) that in the stretched membranes of HEK cells, Nav1.5 exhibits dramatically large irreversible left-shifts {6}.

For an “intact” Hodgkin-Huxley axon with Na/K pumps (internal and external volumes equal: $vol_o=vol_i$), **Fig 2C** plots V_m , E_{Na} and E_K . Prolonged current injection elicits a sustained train of firing that stops when injections stops, after which the pump slowly readjusts the ion gradients. Within a few seconds the system has returned to its initial state. This is the healthy axon’s response to a long stimulus. Below (**Fig 2D**) we see the response of a mildly injured axon. Here, there is current injection. Instead, at $t=0.2$ s, a mild irreversible Nav-CLS injury (all Nav channels shifted by 1.5 mV) is imposed. For >8 s, the previously quiescent axon fires tonically. This “spontaneous” ectopic firing, propagating antero- and retrogradely, would constitutes a seriously neuropathic condition. Note that with this mild Nav-CLS injury, E_{Na} and E_K change due to channel activity then at some point, ectopic firing stops “spontaneously” and several seconds later the injured system settles to a new steady-state. The axon has responded to its small Nav-CLS injury by “left-shifting” its E_K . With more intense and/or extensive Nav-CLS injury, the system’s new steady state is not a fixed V_{rest} but a slow rhythmic pattern of bursts, as seen e.g. in the $vol_o=vol_i$ case of **Fig 2E**. Other simulations in that series demonstrate that bursting particulars change as $vol_o:vol_i$ ratio changes. Severe Nav-CLS (e.g., the 20 mV shift of **Fig 2A**) yields depolarizing block, but even so, window current leak continues dissipating the Na-gradient. A common feature of neuropathic firing in axons is the subthreshold voltage oscillations seen before and after bursts, and over part of the mild injury range, Nav-CLS injury in axons generates those phenomena.

These results in an axon model serve as a heads-up that leaky fast-mode Nav channels in damaged cardiomyocytes (and other excitable cells) may have been overlooked. Even the effectiveness of Nav reagents that bind with higher affinity to slow-mode than fast mode Nav channels is not definitive proof that only slow mode Nav-leak occurs, since these lipophilic compounds might partition better into damaged than intact membrane {52}. Further complicating matters, altering pump activity, inhibiting volume regulatory transporters, inhibiting Kv channels and so on – many such manipulations would change an excitable cell’s abnormal firing pattern (as per **Fig 2E**), even though the origin of a dysrhythmia was in fact Nav-CLS. Moreover, a standard I_{Na} voltage-clamp test for “leaky” Nav channels could be misleading if one expected only slow-mode Nav channels to be problematic; in that case, the expectation is that I_{Na} in the g_{max} zone will increase relative to peak current. Note, however, that with Nav-CLS injury, the ratio of [steady-state I_{Na} at ~ 0 mV] to [peak I_{Na} at ~ 0 mV] *decreases* (see $m^3h(V)$ plot at 0 mV, **Fig 2A**).

But beyond all this, the possibility of left-shifted slow-mode Nav channels in damaged cardiomyocyte membranes needs to be investigated. And the main point here is that if and where there is slow-mode Nav-LS injury, there will almost certainly also be fast-mode Nav-CLS injury.

Reversible and irreversible MS modulation of VGCs. Excitable cells fine tune their firing patterns by modulating their VGCs. Restructuring (“deforming”) the embedding bilayer is one manner in which VGCs become modulated in both healthy and diseased conditions (Morris {51} lists where/when, in the cardiac cells bilayer deformation could occur). To study MS modulation of recombinant and native VGCs, we and others exploit stretch {35}{56}{6} or bilayer reagents. Cholesterol and fatty acids can be added/extracted {20}{21}{70}{9}{40}{65}. Bilayer-disrupting drugs such as propofol may be used, though their attention focuses on clinical actions/side effects {42} rather than how the drugs perturb bilayers {1}. Hydrostatic pressure also deforms bilayers, compressing them laterally to yield thicker more ordered, well-packed bilayers {62}. This may explain (see {54}) how large hydrostatic pressures reversibly decelerate and right-shift the activation (along with the coupled inactivation) of squid axon g_{Na} {12}; originally, because voltage sensors were thought to be sequestered from the bilayer, those findings were interpreted in terms of protein compression. Like membranes under hydrostatic pressure, cholesterol/sphingomyelin-enriched membranes are thicker and more well-ordered (compared to cholesterol-extracted membranes), and this exerts hydrostatic pressure-like effects on Nav and Kv channel gating (slower, more right-shifted activation. Membrane stretch, by contrast, thins, fluidizes and disorders bilayers, eliciting in Nav and Kv1 channels faster, more left-shifted activation. And consistent with all this (see {55}{51}{50}), for HCN2 channels (VGCs that “do things backwards”), stretch causes faster deactivation {41}. In effect, hydrostatic compression and tensile stretch are on a bilayer mechanical continuum.

The issue here is the behaviors of VGCs in membranes of sick excitable cells {49}{52}. Where membrane-skeleton interactions become disrupted, bilayer fluidity is elevated and the bilayer’s healthy asymmetry decays (a genetically induced case: dystrophic membranes {2}{25}{79}). This is “bleb-like” injury, though in mildly injured cells (the potentially salvageable ones) the regions of nascent bleb may be too small and dispersed to be evident by light microscopy. Thus, for bleb-like injury, the areas of VGC-rich bilayer we are most interested in are not the late-stage blebs and vacuoles of apoptotic and necrotic post ischemia/reperfusion cardiomyocytes {29}. Rather we assume that membranes go through a period of nascent-stage bilayer damage, a time before insult-induced bilayer disorder and blebbing are beyond remediation {17}. Bilayer injury along these lines is expected where there is ischemia, where reactive oxygen species are generated, where a mechanical trauma occurs, where inflammatory conditions prevail, and where various genetic or toxic conditions damage the cortical cytoskeleton {47}. For a specific example, cultured porcine cardiomyocytes subjected to ischemia then reperfusion produced blebbing cells within 2 hours of restoring oxygen.

Our findings for Nav1.6 channels {83} crystallized our realization that bleb-inducing stretch injury to cell-attached patches exerts the same class of effect on Nav gating as elastic stretch. In principle, bilayer deformations can be entirely reversible (elastic) or entirely irreversible (plastic). **Fig 1** schematizes this for VGCs making MS-Speed responses and MS-Number responses, terms to be elucidated further as we go along. As also indicated in **Fig 1**, in experiments where $g(V)$ curves are monitored before, during and after an imposed stretch, deformations of complex biological membranes could be “partially reversible” or “partially

plastic” and so on. The before, during and after could in fact refer to any bilayer restructuring perturbation or insult. In the case of stretch, membrane damage could vary from zero (meaning the bilayer deformation was fully elastic) up to some maximum (the deformation was fully plastic). In biomembranes (unlike simple symmetric artificial membranes), plastic deformations of graded intensity are a reasonable expectation. They would explain the progressive irreversible stretch-induced $g_{Na}(V)$ left-shift of Nav channels in stretched membranes [75][83][6][49][52]. Admittedly, there is a possibility that, at the unitary channel level, what happens is an all-or-none (i.e., not graded) left-shift process in which the Nav channel unbinds (or perhaps binds) some modulatory ligand (e.g., ankyrin-G). Whatever the precise left-shift mechanism, irreversible membrane deformations can be said to have “saturated” at the point when increasingly intense stretch elicits no further irreversible change. Thereafter, stretch elicits stretch-intensity dependent elastic responses (**Fig 1**). Prior to this, large plastic changes can easily obscure smaller elastic ones as we now realize occurred in our studies of Nav1.4 in oocytes [75]; we now know (unpublished observations) that like other Nav channels, Nav1.4 shows both plastic and elastic responses to stretch.

To sum up: **a)** whatever the bilayer-deforming factor, reversible bilayer restructuring elicits reversible MS modulation of VGCs, and irreversible restructuring elicits irreversible MS modulation, and **b)** to help determine whether irreversible VGC modulation arises from irreversibly perturbed bilayer structures, also study reversible MS modulation of that VGC in the same system.

The MS behavior of VGCs as a matter of the heart –are cardiac bilayers perturbed?

Sophisticated precision techniques for studying and modeling tissue mechanics in the beating myocardium are becoming available (e.g. [46]), but this does not extend to the nanoscale level of bilayer mechanics, the scale relevant for VGCs and other membrane proteins. Whether elastic membrane deformations occur in cardiac membranes on a beat-to-beat basis or even more chronically in connection with distended atrial and ventricular chambers has not been elucidated. Moreover, assertions about unidentified stretch-activated cation channels notwithstanding, direct evidence that elastic deformations modulate *any* cardiomyocyte ion channel in situ is still lacking, including for the identified and ubiquitous VGCs [51].

The existence of plastic deformations of cardiac bilayers, on the other hand, has been repeatedly extensively confirmed, insofar as plastic changes occur they link to dietary lipids, with developmental/physiological changes, with various pharmacological agents. Or consider a particular VGC species that traffics to both intercalated disc and t-tubular sarcolemmal membranes [16]; surely it “feels” mechanically-different bilayer structures. Likewise for any particular VGC species in caveolar vs non-caveolar bilayer or in raft vs non-raft bilayer [28].

In cases of injury-induced plastic changes in bilayer structure (due to ischemia, inflammation, trauma, toxins [59][23][30] and so on), the general existence of plastic change – bilayer perturbations - is again, not challenged, but information on the nanoscale level specifics of those perturbations is sparse. An exception is a recent study involving rat cardiomyocytes and using laurdan and 1,6-diphenyl-1,3,5-hexatriene to probe membrane fluidity changes [80] elicited by toxic metabolites of pyrethroid. These compounds, which impair VGC function, foster lipid

peroxidation of plasmalemmal bilayers. Laurdan, which produces a signal sensitive to the extent of water penetration into the bilayer's hydrophobic interior, probes the lateral mobility and polarity of its environment, while the 1,6-diphenyl-1,3,5-hexatriene measures fluidity changes in the hydrophobic interior. For exposure to low levels of metabolites (10-20 μ M range) this group observed metabolite-induced membrane fluidity changes that varied with partition coefficient. Those were cellular measurements but, using 2-photon microscopy, laurdan signals can be monitored at small depths into living tissues {60} (e.g., zebrafish embryos). Using these and other fluorescence probes of bilayer fluidity, it might be feasible to monitor changes in individual cardiomyocytes or in cardiac tissues as they were subjected to ischemia, exposed to short-chain alkanols, or stretched and so on.

MS-Speed and MS-Number: kits for putting MS-modulated VGCs into cardiac models.

We can now safely infer that, be they elastic or plastic, bilayer deformations accelerate the major depolarization-induced motions of voltage sensors {34}{67}{50}. But voltage sensor movements are several steps removed from the physiological "currency" of excitable cells, namely the flux of ions through open pores, fluxes that charge/discharge V_m and that mediate $\Delta[Ca^{2+}]_{int}$. Typically, mathematical models of cardiac electrophysiology have as outputs V_m and $[Ca^{2+}]_{int}$ and while unidentified stretch-activated channels are sometimes included in those models {78}, one preliminary study {3} has taken into account the fact that VGCs are ubiquitous and subject to MS modulation {51}. Where the issue is injurious irreversible MS modulation of VGCs, there is an even stronger argument for incorporating MS-modulated VGC behavior in model studies.

To a first approximation, MS modulation of VGCs falls into one of two categories that we characterize as MS-Speed (e.g. Nav and Kv1 channels: currents accelerate, $g(V)$ shifts along the V_m axis, its slope is fixed as is g_{max}) and MS-Number (e.g. VGCa and Kv3 channels: current speed and $g(V)$ midpoint and slope is unaffected but apparent g_{max} increases). These simple descriptors could help with the task of incorporating into cardiac electro-rhythmicity models realistic but computationally tractable descriptions of MS-modulated VGCs. As already described above, the MS-Speed approach we used for Nav channels and axon damage could be modified appropriately for use in cardiac models. That model of injury, however, is inappropriate for Cav channels, which would need a MS-Number approach. To help with computational tool-kits for VGCs in damaged bilayers (or otherwise MS-modulated VGCs), the next section introduces several over-arching concepts. We then discuss them mostly with reference to the MS behavior of a rather uncomplicated VGC, namely Kv3, for which we show some data. Kv3 is useful here because it has VGCa-like MS responses {57}, and because it provides a particularly straightforward way to point out that VGC mode-switch needs to be taken into account when studying MS modulation of VGCs. VGC mode-switching occurs routinely on the beat-to-beat time scale of the myocardium {44}. We encountered the complexities of mode-switch in our studies of the MS modulation of HCN2 {41} and Nav1.6{52}, but, as it happens, mode-switch is both easy-to-grasp by direct inspection of Kv3 currents and not made baffling by MS modulation of the currents.

Some key concepts for understanding MS-Speed and MS-Number modulation of VGCs

a) Rate-limiting voltage-dependent (RLVD) transitions. On the activation pathway of any VGC there is a RLVD step governing the rate of channel opening: that RLVD step may or may not be a MS step. The RLVD step is MS in Nav channels but is not MS in Kv3 or L-type Cav channels (reviewed in {57}). This, in essence, underlies the MS-Speed and MS-Number categories. Given the complexities of VGC kinetics, these are useful, but not “iron-clad”, descriptors for MS modulation.

b) Mode-Switch. During prolonged depolarizations (e.g. several tens of milliseconds) VGCs (having accomplished their voltage-dependent transitions) typically undergo voltage-independent mode-switch transitions {41}; the possibility that some mode-switch transitions are MS needs to be investigated.

c) Chronic MS modulation. Reversible and irreversible responses of VGCs to stretch are qualitatively similar for Nav channels, as if both are due to the thinned/disordered bilayer. It is less clear if this also applies for MS-Number VGCs, but assuming it does, reversible MS modulation studied in biophysical experiments can add to our understanding of the diverse chronic MS-modulations of VGCs.

A special rate-limiting voltage-dependent steps and the MS response of Kv3

Kv3 channels, like L-type Ca channels (based on responses to osmotic swelling and whole-cell inflation (see review in {57})), show MS-Number behavior. Unlike Kv3, $I_{Ca}(V_m, t)$ cannot be studied in stretched oocyte membranes {10}; the lanthanide ions used to inhibit endogenous MS channels block g_{Ca} . Initially, we examined Kv3 expecting it to echo the interesting MS-Speed responses of “ILT”, a biophysical-tool channel {33}. Emphatically, it does not, a reminder that the amino acid dependent functions of a VGC play out in a bilayer context, and that context can be probed via stretch perturbations.

Unlike Shaker-Kv1, with its 4th order activation (like a Hodgkin-Huxley delayed rectifier), Kv3 activation is 1st order kinetics and requires strongly depolarized potentials {36}; Shaw-Kv3 inspired the much-used Shaker-Kv1 mutant Shaker-ILT{32}{61}{14}. In Kv1-ILT, voltage sensors are subtly altered by incorporation of a key 3 amino acid motif of the Kv3 voltage sensor, ILT, but the impact is powerful. In Kv1-WT, gate-charge moves concertedly (4 subunits simultaneously) as a 1st order process at about the same hyperpolarized voltage as the major sensor-charge movements (4 subunits independently). In ILT, however, sensor-charge and gate-charge motions are energetically de-coupled: sensor-charge moves at the normal (hyperpolarized) voltage, but the concerted gate-charge moves only with strong depolarization. Hence, ILT, the concerted gate-motion is the RLVD step governing P_{open} .

We reported the MS-Number responses of Kv3-F335A {33}, and along with data for Kv3-WT and Kv3-P410A, we illustrate that further here. Alcohol-modulated Kv3 gating of these particular channels is studied in the Covarubbias lab, with Kv3-F335A as their experimental-“WT”{70}{24}. With stretch, the P_{open} of F335A increases reversibly (unitary current is unchanged), there is an apparent g_{max} increase and no change in activation speed {33}. With Shaker-ILT, current decelerates with stretch, with g_{max} remaining fixed and the activation curve right-shifts with an unchanging slope {33}. Since the MS responses of ILT and Kv3 are radically

different (MS-Speed vs MS-Number responses), we can assert that a late concerted RLVD step is not a requirement for MS-Number responses.

The next section fleshes out some data on the MS-Number modulation of Kv3.

More Kv3 MS results

The data shown in **Fig 3** and **Fig 4** are described in their legends then and discussed in the next sections extend findings reported previously for Shaw Kv3 channels {33}. The three Kv3 cDNAs were kindly provided by M. Covarubbias (see {70}{24}). Channels were expressed in oocytes at levels that yield macroscopic I_K in well-fire-polished (with a molten soda glass-coated filament {56}) cell-attached patches. Pipette resistances were 2-4 M Ω . Recording conditions were as previously described (high-K⁺ and 1 mM lanthanum in the pipette {41}) with continually monitored pipette pressure used to stress the membrane. Membrane tension is unknown. P/N=4 linear subtraction was used.

Unlike the experiments on Nav1.6 {83} which were done exclusively starting with gently-sealed patches (explained in {56}), the Kv3 experiments were done on patches sealed using ~10-40 mmHg suction. The patched membranes would have undergone considerable plastic (bleb-like) damage by the point that recordings began. In retrospect, for these MS-Number channels, an initial plastic damage stage that might have been routine had we used gently sealed patches would likely have been interpreted by us as a somewhat annoying and mysterious “run-up”: more channels (Number) appearing from “nowhere” with normal kinetics. As will be seen below, this makes good biophysical sense for VGCs with MS-Number responses. A cautionary note, therefore: run-up of VGCs in patch recordings (and in whole cell recordings where, as often happens, cells slowly inflate) might in some cases coincide temporally and mechanistically with onset of bleb-like membrane damage.

Mode-switch – Kv3 fits the pattern

For WT Kv3 and the two point-mutants, **Fig 3A** illustrates that in response to depolarizing steps from -100 mV, 150 ms I_K traces are well-described by the sum of two first order exponentials. Although, as expected {36}, the first ~10 ms is well fit by a single exponential, we maintained the step depolarization to 150 ms, and under those circumstances, sums of two exponentials were required. The Kv3 tail currents (upon repolarization after 150 ms) moreover, follow two-exponentials decay processes (**Fig 3B**). Evidently the Kv3 channels have two open states. The pattern of activation/deactivation involving two open states would be consistent with the mode-switch scheme sketched in **Fig 5A**. This scheme is based on the Active-Mode/Relaxed-Mode model proposed by Bezanilla and colleagues for all VG proteins {81}. VG phosphatases {81}, HCN channels {44} and Nav channels {38}{52}, e.g., all exhibit voltage dependent (VD) activation/deactivation and voltage-independent (VI) mode-switch behaviors along this line. An example of such mode-switching in action in a cardiac physiology context is seen through modeling of sinoatrial cell action potentials by Mannikko and colleagues {44}. Ramp currents for recombinant HCN2 channel before/during and after stretch, as seen in **Fig 5Biii**, show that hysteresis (a manifestation of mode-switch) is not abolished by stretch.

We prefer the term “mode-SWITCH” to mode-shift {41}{52}. Switch better evokes a discrete conformation change in the voltage-sensor (i.e., a VI transition or “switch” from Active-Mode to Relaxed-Mode or vice versa). When an open Kv or Nav (or, for HCN, closed) channel in Active-Mode undergoes a mode-switch, it enters a lower energy Relaxed-Mode state {81}.

The scheme of **Fig 5A** posits that in hyperpolarized membranes, Kv3 channels accumulate near the C_A states but with prolonged depolarization would accumulate near the O_R state. Steady-state I_K for Kv3 would thus be a mix of O_R and O_A , with the double exponential tail currents representing deactivations from both states.

An aside on “sites”: chemical and physical MS modulation of Kv3 and other VGCs

In oocyte membranes, inhibition of Kv3 steady-state I_K has been examined for short chain 1-alkanol over a range of concentrations by Covarrubias and colleagues {70}. In solvent-free bilayers (such as the oocyte membrane), short chain alkanols cause chain-length dependent thinning, they increase bilayer disorder and they reduce surface tension {43}{20}. They govern steady-state Kv3 P_{open} in accordance with this pattern, without dose-saturation or stereospecificity. Clearly, Kv3 channels feel bilayer deformations {33} but the mechanosensitivity of Kv3 channels is discounted in models that see alcohols and general anesthetics as ligands acting on them at specific protein-based binding sites {5}. If alcohols do indeed destabilize the Kv3 open state (the two states, in fact, as seen here) via allosteric actions at an entirely protein-based binding site, it remains true that the entity being modulated resides in an alcohol-perturbed bilayer structure {27}. As stressed by Mackinnon and colleagues {68} molecular models that invoke channel structure need to factor in the bilayer constituents as part of the energetics of P_{open} (or, as here, $P_{(O_A+O_R)}$). For lipidic constituents present in sufficient quantity to perturb the peri-VGC bilayer structure, as well as for countless amphiphilic drugs that produce VGC side effects, MS modulation is a more plausible explanation than low affinity binding at hydrophobic “sites” or “pockets” (see {55}{65}). It is useful to think about MS modulation in the following way: the entire structured lateral interface between VGCs and the bilayer leaflets {63} is in effect an “allosteric effector site” for VGC motions {49}.

Rate-limiting voltage dependent steps: is the RLVD transition an MS transition?

Among different VGC species, the precise ways in which voltage sensor motions regulate ion-current flow differ. By definition, any motion of a voltage sensor through the electric field will be voltage-dependent (VD) and where a VD sensor motion also “feels bilayer deformations, it will be a MS-VD motion. However, a portion of a sensor’s total VD movement could occur buried in the protein in a way that rendered it insensitive to bilayer deformations. This presumably explains why the RLVD activation step in Kv3 and Cav channels {10} is not a MS transition. In the scheme of **Fig 5A**, the Kv3 channel MS transition(s) would lie somewhere on the left (in other words, they would be hidden Markov transitions in the “ $C_A..C_A$ ” and/or “ $C_R..C_R$ ” zone). It should be noted that a VGC could also have MS-VI transitions. A slow inactivation process (presumably P-type) in Shaker Kv1-5aa is one example {34} and an anomalous mode-conversion seen in oocytes with α Nav1.4 {75} is also a possible candidate for a MS-VI mode-switch transition.

Thus, the slowest VD step along the path to “open” -- the RLVD step -- may or may not be a MS step. For VGCs whose RLVD step is a MS step, bilayer deformations will accelerate (as in Nav1.5{4}) or decelerate (as in Kv1-ILT) the activation process thus left- or right-shifting $g(V)$. When the bilayer surround of say, a Nav channel, is reversibly disordered/thinned/fluidized (by stretch, by fluidizing agents) $I_{Na}(t)$ reversibly accelerates for all values of V_m (e.g. Fig 1C of{54} and Fig 3D of {4} show stretch-accelerated activation at V_m levels where g_{max} has already been attained). But for an L-type Cav channel, whose RLVD step (like that of Kv3) is a non-MS transition, $I_{Ca}(t)$ for all values of V_m scales up by the same amount. This translates to apparent g_{max} increasing by that scaling factor. The mechanosensitivity or not of the RLVD transition thus provide a general explanation for the two categories of MS modulated VGC behavior, “MS-Speed” and “MS-Number”.

Similarities in reversible and irreversible MS responses: from biophysics to pathology

Reversible stretch modulation of VGCs signifies elastic changes in bilayer structure {22}{76}{41}{54} but to assign mechanisms for irreversible stretch-modulation of VGCs is more difficult {75}{69}{56}. What is clear is that use of pipette aspiration to stretch membranes causes progressive bleb-like damage {53}{72}{82}{49}{87}{71}{74}. Saturation of plastic deformation is defined operationally by the point when the embedded channels respond reversibly to what are then assumed to be elastic deformations. The behavior with Nav1.6 in oocytes (see Fig 5 in {83}) and other Nav isoforms exemplify the plastic-elastic diagram of **Fig 1, MS-Speed** is appropriate.

The equivalent diagram for MS-Number channels is in agreement with our findings for N-type Cav channels in HEK cells {10}. Concomitant I_{Ca} and video recording involving whole-cell inflation revealed that MS-Number responses (increased g_{max}) occurred abruptly at a point when the inflation pressure caused bleb-like damage. In unitary channel recordings from cell-attached patches (small tips, large gigaohm seals, and hence, unavoidably, perturbed bilayer) we obtained reversible stretch-induced “ iNP_{open} ” increases. This was attributed to increased N (number of participating channels), not increased unitary current (i) or and not a changed open duration for unitary events (the conditional P_{open}). For these VGCa channels, therefore, the plastic-elastic diagram seems appropriate and valid. Ionic and gating currents of recombinant L-type cardiac Cav channels (obtained from cut-open oocytes) reveals that the coupling efficacy between voltage sensor charge movement and pore opening in these channels is facilitated by prolonged prepulse depolarizations {13}, with no change in $I_{Ca}(t)$ kinetics. In effect, the apparent g_{max} increases with prepulse depolarizations, just as it does with membrane stretch. Leaky Cav channels (and ryanodine receptors) in ischemically damaged cardiomyocytes are important drug targets {26}{19}. For those concerned with the underlying mechanisms of Cav-leak, a key question, we suggest, is this: does bleb-like membrane damage of cardiomyocyte membrane elicit an irreversible increase in apparent g_{max} ? If so, damage should irreversibly left-shift the gating charge curve ($Q(V)$); debilitation instead of facilitation.

Consider cardiac Nav1.5 in rat ventricular myocytes. In spite of difficulty maintaining patches, we managed to demonstrate that the native Nav1.5 exhibits elastic MS-Speed behavior {4}. It is also clear from the work of Beyder and colleagues {6} that Nav1.5 channels patch-

stretched in HEK cells show extensive plastic MS-Speed responses. It is only reasonable, therefore to predict that Nav1.5 (slow- and fast-gating) in native membranes with bleb-like injury (from ischemia, from inflammation, from an abrupt mechanical blow) would show MS-Speed type Nav-leak.

In oocyte patches, the MS-Number responses of Kv3 channels were largely reversible (as mentioned above, seal formation was done with intense pipette aspiration). Nevertheless, when irreversible change was noted it followed the MS-Number pattern of the elastic responses, as illustrated by **Fig 4**. For that patch, currents (illustrated in **A**) were repeatedly acquired without and with stretch (suction or blowing) until the patch ruptured, as summarized by the histogram, **B**. Stretch reversibly increased apparent g_{max} , with the most intense suction (-70 mmHg) yielding the biggest reversible increase. And, consistent with the MS-Number responses that showed no change in kinetics (voltage step experiments (**Fig 3**)), normalized $I_K(t)$ for these ramp-then-hold traces (without/with stretch) superimpose. However, as evident from the “upward” trend of 0 mmHg levels in the histogram, apparent g_{max} at 0 mmHg almost doubled. Normalized I/V traces for the first and last 0 mmHg ramps overlap perfectly (**Fig 4C**), consistent with this plastic change being mechanistically comparable to the elastic change, i.e. a MS-Number response. It will be interesting to re-assess whether L-type Ca channels in cardiomyocytes are

Conclusions

VGCs are multi-conformation membrane proteins whose voltage sensors interact extensively with the channel’s embedding bilayer. VGCs thus cannot both gate and remain entirely indifferent to the mechanical state of the bilayer in which they are embedded; voltage sensors must do work on the bilayer in order to repack. In the myocardium, VGCs never see an unchanging voltage, so “bad bilayer mechanics” can be expected to be arrhythmia-inducing.

If the bilayer is more fluid/disorderly/thin at one time than another, then voltage sensors will move more easily under those conditions than at another time when the bilayer is more solid-like, well-packed or thicker. In principle, a bilayer might alternate between these two extremes reversibly (in an elastic fashion) or irreversibly (in a plastic fashion). Either way, VGCs will respond. And because different species of VGCs couple their sensor motions to gate opening differently, responses to perturbed bilayer structure plays out differently in different VGCs. For most VGCs, this simplifies down to saying that either activation speeds up or the apparent number of open channels increases.

The plastic bilayer perturbations are expected to occur in cardiomyocytes subjected to ischemic, inflammatory and other conditions. For axonal Nav channels, we showed that taking the plastic changes seriously in the context of a mildly damaged axons yields ectopic firing patterns typical of peripheral neuropathies.

We characterize MS-modulation of diverse VGCs under two categories in hope that this will help cardiac experimentalists and modelers re-examine the “leaky” VGCs in acquired cardiac disease states to determine if they are indeed manifestations of plastic MS-modulation responses we describe here.

Many clinically promising or useful VGC inhibitors are lipophilic {45}{38}. As such, they might partition differently into healthy, well-packed bilayers than into damaged-fluidized (bleb-like) bilayers. In cases where the leaky VGCs targeted by lipophilic inhibitors are MS-modulated VGCs in damaged bilayers, there might be opportunities to optimize targeting. To reduce unwanted inhibition of non-leaky VGCs in healthy membrane, the drug could be modified to ensure that its specific binding to the VGC-site is most effective in fluidized bilayers. Increasing the drug's partition coefficient for fluidized VGC-rich bilayers (relative to healthy bilayers) would also enhance selectivity. In a perverse fashion, nature seems to take this general approach in spider venoms, where toxic amphiphilic peptides are accompanied by membrane-fluidizing lipases. The toxic peptides target binding sites on voltage sensors, but their efficacy as VGC inhibitors is greatly improved when the embedding bilayer becomes fluidized {50}{52}.

FIGURE LEGENDS (*repeated adjacent to the figures*)

Figure 1 VCC activation and membrane stretch: MS-Speed and MS-Number responses. MS-Speed: shifts along the V_m -axis. MS-Number: a change in the apparent g_{max} . For stretch at a given intensity, $g(V)$ change can be reversible, partially reversible, or irreversible (before (black), during (red) and after stretch (grey)). In response to progressively increasing stretch intensity, $g(V)$ curves for VGCs in an intact membrane go through a range of plastic (irreversible) change which saturates at some point, after which stretch-intensity dependent reversible changes can be recorded without interference from concurrent irreversible change.

Figure 2 Nav-CLS injury and ectopic excitation. **A.** Hodgkin-Huxley $m^3(V)$ and $h(V)$ plots for control conditions and with 20 mV hyperpolarizing (left) shifts; below, their steady-state products (window conductances). **B.** As explained in the text, i) irreversible response of recombinant Nav1.6 current to stretch, and ii) illustration of a 20 mV coupled left-shift. **C, D, E.** Computational results for a mildly traumatized axon, as described in the text. Expanded time resolution is provided in 3 instances to show action potential shapes. In **E**, the Nav-CLS injury (2 mV, all Nav channels) is the same in every case, with the only difference in the simulations being the different volume ratios $vol_o:vol_i$, as indicated by the numbers 0.1, 0.5, 1.0, 3 and 4.

Figure 3 Kv3 channel kinetics without and with stretch: two open states and MS-Number responses. **A, B** Typical activation and tail current traces for Shaw Kv3 WT, F335A and P410A channels with overlaid fits (green) to sums of two exponentials. **C, D** For WT and P410A, traces before, during, after stretch (black, red, grey as per $g(V)$ relations of Fig 1) and at right for each, the average of before+after traces amplitude-normalized to the during-stretch trace. The complete overlap signifies that there has been no effect on kinetics, what changes with stretch is the number of channels participating; the Kv3 response to stretch appears to be comparable to the facilitating effect of pre-pulse depolarizations on cardiac L-type VGCa channels {13} where increased efficacy of coupling between sensor charge movement and pore opening is responsible.

Figure 4 MS-Number behavior in Shaw Kv3 F335A using ramp-then-hold clamp. **A,** A series of before/during/after stretch traces with stretch applied by pipette aspiration (suction) at the intensity shown (mmHg). The voltage protocol: from $V_{hold}=-100$ mV, a 500 ms ramp to -120 mV and after 120 ms there, back to V_{hold} . (panel C labels these). Note that the I_K plateaus do *not* represent a g_{max} condition. They provide steady-state I_K at +120 mV (i.e. the y-axis in **B**). Note different current scales. Also note that by ~-40 mmHg and beyond, stretch-modulated I_K exceeds depolarization-induced I_K . **B,** histogram summarizing the “stretch-dose” response experiment from which these traces are taken, with black=0 mmHg controls. In **C**, the first and last 0 mmHg traces are plotted then normalized (procedure as in Fig 3), and in **D, E** the full traces for -20 mmHg (first time) and +20 mmHg are plotted then normalized, illustrating MS-Number behavior as seen for ramp-then-hold currents and illustrating that blowing into the pipette is the equivalent of applying suction, as expected when increased bilayer tension is the modulating factor.

Figure 5 Mode-switch and MS modulation of VGCs. A, simplified scheme for Kv3 channels in closed/open (C,O) active/relaxed (A,R) mode states connected by voltage-dependent (VD) and voltage-independent (VI) transitions (the latter being the mode-switch transitions). In Kv3, VD transitions (and thus gating current motions) must occur between closed states indicated on the left of the diagram, but those transitions are not rate-limiting for pore opening. At least one must be a MS transition that augments the fraction of channels “ready-to-open-upon-depolarization”. This scheme is directly analogous to the mode-switch scheme used for HCN2 channels, {41}; it is redrawn in **Bi** with the naming and color conventions of **A**. In both schemes, prolonged hyperpolarization causes channels to populate states near the orange diamond while prolonged depolarization causes channels to populate near the blue diamond. Both are also analogous to a simplified mode-switch scheme for Nav channels {52}. **Bii, iii** illustrate the sawtooth ramp protocol (it includes first a fast, **f**, then a slower, **s**, voltage sawtooth) used to elicit the characteristic mode-switch-induced hysteresis of HCN2 cation currents elicited before, during, after stretch (modified from {41}).

REFERENCES

- [1] Ali, M.H., Kirby, D.J., Mohammed, A.R., Perrie, Y. 2010. Solubilisation of drugs within liposomal bilayers: alternatives to cholesterol as a membrane stabilising agent. *J. Pharm. Pharmacol.* 62, 1646-55.
- [2] Allen, D.G., Zhang, B.T., Whitehead, N.P. 2010. Stretch-induced membrane damage in muscle: comparison of wild-type and mdx mice. *Adv. Exp. Med. Biol.* 682, 297-313.
- [3] Banderali, U., Clark, R.B., Morris, C.E., Fink, M., Giles, W.R. 2010. Effects of applied stretch on native and recombinant cardiac Na⁺ currents. In: *Mechanosensitivity in Cells and Tissues: Mechanosensitivity of the Heart*, Kamkin A., Kiseleva I. (eds), Springer pp 169-184
- [4] Banderali, U., Juranka, P.F., Clark, R.B., Giles, W.R., Morris, C.E. 2010. Impaired stretch modulation in potentially lethal cardiac sodium channel mutants. *Channels (Austin)*. 4, 12-21.
- [5] Barber, A.F., Liang, Q., Amaral, C., Treptow, W., Covarrubias M. 2011. Molecular mapping of general anesthetic sites in a voltage-gated ion channel. *Biophys. J.* 101, 1613-22.
- [6] Beyder, A., Rae, J.L., Bernard, C., Stregue, P.R., Sachs, F., Farrugia, G. 2010. Mechanosensitivity of Nav1.5, a voltage-sensitive sodium channel. *J. Physiol.* 588, 4969-85.
- [7] Bouchard, S., Jacquemet, V., Vinet, A. 2011. Automaticity in acute ischemia: bifurcation analysis of a human ventricular model. *Phys. Rev. E Stat. Nonlin. Soft Matter Phys.* 83, 011911.
- [8] Boucher, P.A., Joós, B., and Morris, C.E. 2012. Coupled left-shift of Nav channels: modeling the Na⁺-loading and dysfunctional excitability of damaged axons. (Revised manuscript at) *J. Comput. Neurosci.*
- [9] Bruno, M.J., Koeppe, R.E., Andersen, O.S. 2007. Docosahexaenoic acid alters bilayer elastic properties. *Proc. Natl. Acad. Sci. USA* 104, 9638-43.
- [10] Calabrese, B., Tabarean, I.V., Juranka, P., Morris, C.E. 2002. Mechanosensitivity of N-type calcium channel currents. *Biophys J.* 83, 2560-74.
- [11] Charras, G., Paluch, E. 2008. Blebs lead the way: how to migrate without lamellipodia. *Nat Rev Mol Cell Biol.* 9, 730-6.
- [12] Conti, F., Fioravanti, R., Segal, J.R., Stühmer, W. J. 1982. Pressure dependence of the sodium currents of squid giant axon. *Membr Biol.* 69, 23-34.
- [13] Costantin, J.L., Qin, N., Zhou, J., Platano, D., Birnbaumer, L., Stefani, E. 1998. Long lasting facilitation of the rabbit cardiac Ca²⁺ channel: correlation with the coupling efficiency between charge movement and pore opening. *FEBS Lett.* 423, 213-7.
- [14] del Camino, D., Kanevsky, M., Yellen, G. 2005. Status of the intracellular gate in the activated-not-open state of shaker K⁺ channels. *J Gen Physiol.* 126, 419-28.
- [15] DiFrancesco, D., Borer, J.S. 2007. The funny current: cellular basis for the control of heart rate. *Drugs.* 67 (Suppl) 2, 15-24.

- [16] Domínguez, J.N. , de la Rosa, A., Navarro, F., Franco D., Aránega A.E. 2008. Tissue distribution and subcellular localization of the cardiac sodium channel during mouse heart development. *Cardiovasc. Res.* 78, 45-52.
- [17] Draeger, A., Monastyrskaya, K., Babiychuk, E.B. 2011. Plasma membrane repair and cellular damage control: the annexin survival kit. *Biochem. Pharmacol.* 81, 703-12.
- [18] Du, Y.M., Nathan, R.D. 2007. Simulated ischemia enhances L-type calcium current in pacemaker cells isolated from the rabbit sinoatrial node. *Am J Physiol Heart Circ Physiol.* 293, H2986-94.
- [19] Fauconnier, J., Meli, A.C., Thireau, J., Roberge, S., Shan, J., Sassi, Y., Reiken, S.R., Rauzier, J.M., Marchand, A., Chauvier, D., Cassan, C., Crozier, C., Bideaux, P., Lompré, A.M., Jacotot, E., Marks, A.R., Lacampagne, A. 2011. Ryanodine receptor leak mediated by caspase-8 activation leads to left ventricular injury after myocardial ischemia-reperfusion. *Proc. Natl. Acad. Sci. U S A.* 108, 13258-63.
- [20] Finol-Urdaneta, R.K., McArthur, J.R., Juranka, P.F., French, R.J., Morris, C.E. 2010. Modulation of KvAP unitary conductance and gating by 1-alkanols and other surface active agents. *Biophys. J.* 98, 762–72
- [21] Ganapathi, S.B., Fox, T.E., Kester, M., Elmslie, K.S. Ceramide modulates HERG potassium channel gating by translocation into lipid rafts. 2010. *Am. J. Physiol. Cell. Physiol.* 299, C74-86.
- [22] Gu, C.X., Juranka, P.F., Morris, C.E. 2001. Stretch-activation and stretch-inactivation of Shaker-IR, a voltage-gated K⁺ channel. *Biophys. J.* 80, 2678-93.
- [23] Haeseler, G., Foadi, N., Wiegand, E., Ahrens, J., Krampfl, K., Dengler, R., Leuwer, M. 2008. Endotoxin reduces availability of voltage-gated human skeletal muscle sodium channels at depolarized membrane potentials. *Crit. Care Med.* 36, 1239-47
- [24] Harris, T., Graber, A.R., Covarrubias, M. Allosteric modulation of a neuronal K⁺ channel by 1-alkanols is linked to a key residue in the activation gate. 2003. *Am. J. Physiol. Cell. Physiol.* 285, C788-96.
- [25] Hirn, C., Shapovalov, G., Petermann, O., Roulet, E., Ruegg, U.T. 2008. Nav1.4 deregulation in dystrophic skeletal muscle leads to Na⁺ overload and enhanced cell death. *J. Gen. Physiol.* 132, 199-208.
- [26] Hu, X., Wu, B., Wang, X., Xu, C., He, B., Cui, B., Lu, Z., Jiang, H. 2011. Minocycline attenuates ischemia-induced ventricular arrhythmias in rats. *Eur J Pharmacol.* 654, 274-9
- [27] Ingólfsson, H.I., Andersen, O.S. 2011. Alcohol's effects on lipid bilayer properties. *Biophys. J.* 101, 847-55.
- [28] Kaiser, H.J., Lingwood, D., Levental, I., Sampaio, J.L., Kalvodova, L., Rajendran, L., Simons, K. 2009. Order of lipid phases in model and plasma membranes. *Proc Natl Acad Sci U S A.* 106, 16645-50
- [29] Khanal, G., Chung, K., Solis-Wever, X., Johnson, B., and Pappas, D. 2011. Ischemia/reperfusion injury of primary porcine cardiomyocytes in a low-shear microfluidic culture and analysis device. *Analyst.* 136, 3519-26.
- [30] Klöckner, U., Rueckschloss, U., Grossmann, C., Ebelt, H., Müller-Werdan, U., Loppnow, H., Werdan, K., Gekle, M. 2011. Differential reduction of HCN channel activity by various types of lipopolysaccharide. *Mol. Cell. Cardiol.* 51, 226-35.

- [31] Krepiy, D., Mihailescu, M., Freitas, J.A., Schow, E., Worcester, D., Gawrisch, K., Tobias, D.J., White, S.H., Swartz, K. 2009. Structure and hydration of membranes embedded with voltage-sensing domains. *Nature* 462, 473–79.
- [32] Lacroix, J.J., Bezanilla, F. 2011. Control of a final gating charge transition by a hydrophobic residue in the S2 segment of a K⁺ channel voltage sensor. *Proc. Natl. Acad. Sci. U S A.* 108, 6444-9.
- [33] Laitko, U., Juranka, P.F., Morris, C.E. 2006. Membrane stretch slows the concerted step prior to opening in a K_v channel. *J. Gen. Physiol.* 127, 687-701.
- [34] Laitko, U., Morris, C.E. 2004. Membrane tension accelerates rate-limiting voltage-dependent activation and slow inactivation steps in a Shaker channel. *J. Gen. Physiol.* 123, 135-54.
- [35] Langton, P.D. 1993. Calcium channel currents recorded from isolated myocytes of rat basilar artery are stretch sensitive. *J. Physiol.* 471, 1-11.
- [36] Ledwell, J.L., Aldrich, R.W. 1999. Mutations in the S4 region isolate the final voltage-dependent cooperative step in potassium channel activation. *J. Gen. Physiol.* 113, 389-414.
- [37] Lei, M., Jones, S.A., Liu, J., Lancaster, M.K., Fung, S.S., Dobrzynski, H., Camelliti, P., Maier, S.K., Noble, D., Boyett, M.R. 2004. Requirement of neuronal- and cardiac-type sodium channels for murine sinoatrial node pacemaking. *J. Physiol.* 559, 835-48.
- [38] Lenkey, N., Karoly, R., Epresi, N., Vizi, E., Mike, A. 2011. Binding of sodium channel inhibitors to hyperpolarized and depolarized conformations of the channel. *Neuropharmacology.* 60, 191-200.
- [39] Létienne, R., Bel, L., Bessac, A.M., Vacher, B., Le Grand, B. 2009. Myocardial protection by F 15845, a persistent sodium current blocker, in an ischemia-reperfusion model in the pig. *Eur. J. Pharmacol.* 624, 16-22.
- [40] Li, G.R., Sun, H.Y., Zhang, X.H., Cheng, L.C., Chiu, S.W., Tse, H.F., Lau, C.P. 2009. Omega-3 polyunsaturated fatty acids inhibit transient outward and ultrarapid delayed rectifier K⁺ currents and Na⁺ current in human atrial myocytes. *Cardiovasc. Res.* 81, 286-93.
- [41] Lin, W., Laitko U., Juranka P.F., Morris C.E. 2007. Dual stretch responses of mHCN2 pacemaker channels: accelerated activation, accelerated deactivation. *Biophys. J.* 92, 1559–1572.
- [42] Liu, Q., Kong, A.L., Chen, R., Qian, C., Liu, S.W., Sun, B.G., Wang, L.X., Song, L.S., Hong, J. 2011. Propofol and arrhythmias: two sides of the coin. *Acta. Pharmacol. Sin.* 32, 817-23.
- [43] Ly, H.V., Longo, M.L. 2004. The influence of short-chain alcohols on interfacial tension, mechanical properties, area/molecule, and permeability of fluid lipid bilayers. *Biophys. J.* 87, 1013-33.
- [44] Männikkö, R., Pandey, S., Larsson, H.P., Elinder, F. 2005. Hysteresis in the voltage dependence of HCN channels: conversion between two modes affects pacemaker properties. *J. Gen. Physiol.* 125, 305-26.
- [45] Mason, R.P. 1993. Membrane interaction of calcium channel antagonists modulated by cholesterol. Implications for drug activity. *Biochem. Pharmacol.* 45, 2173-83.
- [46] Matsumoto, K., Tanaka, H., Tatsumi, K., Miyoshi, T., Hiraishi, M., Kaneko, A., Tsuji, T., Ryo, K., Fukuda, Y., Yoshida, A., Kawai, H., Hirata, K.I. 2012. Left Ventricular dyssynchrony using three-dimensional

speckle-tracking imaging as a determinant of torsional mechanics in patients with idiopathic dilated cardiomyopathy. *Am. J. Cardiol.* Jan 27 (epub).

[47] McGinn, M.J., Kelley, B.J., Akinyi, L., Oli, M.W., Liu, M.C., Hayes, R.L., Wang, K.K.W., Povlishock, J.T. 2009. Biochemical, structural, and biomarker evidence for calpain-mediated cytoskeletal change after diffuse brain injury uncomplicated by contusion. *J. Neuropathol. Exp. Neurol.* 68, 241-9.

[48] Moreno, J.D., Clancy, C.E. 2012. Pathophysiology of the cardiac late Na current and its potential as a drug target. *J. Mol. Cell. Cardiol.* Dec 16 (epub).

[49] Morris, C.E. 2011a. Why are so many ion channels mechanosensitive, in *Cell Physiology Source Book*, 4th Ed., Sperelakis N. (ed.), Elsevier, pp 493-505.

[50] Morris, C.E. 2011b. Voltage-gated channel mechanosensitivity. Fact or friction? *Front. Physiol.* 2:25.

[51] Morris, C.E. 2011c. Pacemaker, potassium, calcium, sodium: stretch modulation of the voltage-gated channels. In *Cardiac Mechano-Electric Coupling and Arrhythmias*, 2nd Edn, Kohl, P., Sachs, F., Franz, M.R., (eds.), Oxford University Press, pp 42-9.

[52] Morris, C.E., Boucher, P.-A., Joós, B. 2012. Left-shifted Nav channels in trauma-damaged bilayer: primary targets for neuroprotective Nav antagonists? *Frontiers in Pharmacology*, accepted.

[53] Morris, C.E., Horn, R. 1991. Failure to elicit neuronal macroscopic mechanosensitive currents anticipated by single-channel studies. *Science.* 251,1246-9.

[54] Morris, C.E., Juranka, P.F. 2007a. Nav channel mechanosensitivity: activation and inactivation accelerate reversibly with stretch. *Biophys. J.* 93, 822-33.

[55] Morris, C.E., Juranka, P.F. 2007b. Lipid stress at play: mechanosensitivity of voltage-gated channels. *Current Topics in Membranes* 59, 297-337.

[56] Morris, C.E., Juranka, P.F., Lin, W., Morris, T.J., Laitko, U. 2006. Studying the mechanosensitivity of voltage-gated channels using oocyte patches. *Methods Mol. Biol.* 322, 315-29.

[57] Morris, C.E., Laitko, U. 2005. The mechanosensitivity of voltage-gated channels may contribute to cardiac mechano-electric feedback. In *Cardiac Mechano-Electric Feedback and Arrhythmias: from Pipette to Patient*. Kohl, P., Sachs, F., Franz, M. (Eds.) Elsevier Saunders. pp 33-41.

[58] Mottram, A.R., Valdivia, C.R., Makielski, J.C. 2011. Fatty acids antagonize bupivacaine-induced I_{Na} blockade. *Clin. Toxicol. (Phila.)*. 49, 729-33.

[59] Novak, K.R., Nardelli, P., Cope, T.C., Filatov, G., Glass, J.D., Khan, J., Rich, M.M. 2009. Inactivation of sodium channels underlies reversible neuropathy during critical illness in rats. *J. Clin. Invest.* 119, 1150-8.

[60] Owen, D.M., Rentero, C., Magenau, A., Abu-Siniyeh, A., Gaus, K. 2011. Quantitative imaging of membrane lipid order in cells and organisms. *Nat. Protoc.* 7, 24-35.

[61] Pathak, M., Kurtz, L., Tombola, F., Isacoff, E. 2005. The cooperative voltage sensor motion that gates a potassium channel. *J. Gen. Physiol.* 125, 57-69.

- [62] Periasamy, N., Teichert, H., Weise, K., Vogel, R.F., Winter R. 2009. Effects of temperature and pressure on the lateral organization of model membranes with functionally reconstituted multidrug transporter LmrA. *Biochim. Biophys. Acta.* 1788, 390-401.
- [63] Phillips, R., Ursell, T., Wiggins, P., Sens, P. 2009. Emerging roles for lipids in shaping membrane-protein function. *Nature* 459, 379-85.
- [64] Remme, C.A., Bezzina, C.R. 2010. Sodium channel (dys)function and cardiac arrhythmias. *Cardiovasc. Ther.* 28, 287-94.
- [65] Rusinova, R., Herold, K.F., Sanford, R.L., Greathouse, D.V., Hemmings, H.C. Jr, Andersen, O.S. 2011. Thiazolidinedione insulin sensitizers alter lipid bilayer properties and voltage-dependent sodium channel function: implications for drug discovery. *J. Gen. Physiol.* 138, 249-70.
- [66] Schafer, D.S., Jha, S., Liu, F., Akella, T., McCullough, L.D., Rasband, M.N. 2009. Disruption of the axon initial segment cytoskeleton is a new mechanism for neuronal injury. *J. Neurosci.* 29, 13242–54.
- [67] Schmidt, D., MacKinnon, R. 2008. Voltage-dependent K^+ channel gating and voltage sensor toxin sensitivity depend on the mechanical state of the lipid membrane. *Proc. Natl. Acad. Sci. USA* 105, 19276–81.
- [68] Schmidt, D., Cross, S.R., MacKinnon, R.A. 2009. Gating model for the archeal voltage-dependent K^+ channel KvAP in DPhPC and POPE:POPG decane lipid bilayers. *J. Mol. Biol.* 390, 902-12.
- [69] Shahidullah, M., Harris, T., Germann, M.W., Covarrubias M. 2003. Molecular features of an alcohol binding site in a neuronal potassium channel. *Biochemistry.* 42, 11243-52.
- [70] Shcherbatko, A., Ono, F., Mandel, G., Brehm, P. 1999. Voltage-dependent sodium channel function is regulated through membrane mechanics. *Biophys. J.* 77, 1945-59.
- [71] Sheetz, M.P., Sable J.E., Döbereiner, H.G. 2006. Continuous membrane cytoskeleton adhesion requires continuous accommodation to lipid and cytoskeleton dynamics, *Annu. Rev. Biophys. Biomol. Struct.* 35, 417-434.
- [72] Small, D.L., Morris, C.E. 1994. Delayed activation of single mechanosensitive channels in *Lymnaea* neurons. *Am. J. Physiol.* 267, C598-606.
- [73] Smith, D.H., Meaney, D.F., Shull, W.H. 2003. Diffuse axonal injury in head trauma. *J. Head Trauma Rehabil.* 18, 307-16.
- [74] Suchyna, T.M., Markin, V.S., Sachs, F. 2009. Biophysics and structure of the patch and the gigaseal. *Biophys. J.* 97, 738-47.
- [75] Tabarean, I.V., Juranka, P., Morris, C.E. 1999. Membrane stretch affects gating modes of a skeletal muscle sodium channel. *Biophys. J.* 77, 758-74.
- [76] Tabarean, I.V., Morris, C.E. 2002. Membrane stretch accelerates activation and slow inactivation in Shaker channels with S3-S4 linker deletions. *Biophys. J.* 82, 2982-94.
- [77] Taddese, A., Bean, B.P. 2002. Subthreshold sodium current from rapidly inactivating sodium channels drives spontaneous firing of tuberomammillary neurons. *Neuron* 33, 587–600.

- [78] Trayanova, N.A., Constantino, J., Gurev, V.. 2010. Models of stretch-activated ventricular arrhythmias. *J. Electrocardiol.* 43, 479-85.
- [79] Tuazon, M.A., Henderson, G.C. 2011. Fatty acid profile of skeletal muscle phospholipid is altered in mdx mice and is predictive of disease markers. *Metabolism.* Dec 28 (epub).
- [80] Vadhana, D., Carloni, M., Fedeli, D., Nasuti, C., Gabbianelli, R. 2011. Perturbation of rat heart plasma membrane fluidity due to metabolites of permethrin insecticide. *Cardiovasc Toxicol.* 11, 226-34.
- [81] Villalba-Galea, C.A., Sandtner, W., Starace, D.M., Bezanilla, F. 2008. S4-based voltage sensors have three major conformations. *Proc. Natl. Acad. Sci. USA* 105, 17600-07.
- [82] Wan, X., Juranka, P., Morris, C.E. 1999. Activation of mechanosensitive currents in traumatized membrane. *Am. J. Physiol.* 276, C318-27.
- [83] Wang, J.A, Lin, W., Morris, T., Banderali, U., Juranka, P.F, Morris, C.E. 2009. Membrane trauma and Na⁺ leak from Nav1.6 channels. *Am. J. Physiol. Cell Physiol.* 297, C823-34.
- [84] Weiss, S., Benoist, D., White, E., Teng, W., Saint, D.A. 2010. Riluzole protects against cardiac ischaemia and reperfusion damage via block of the persistent sodium current. *Br. J. Pharmacol.* 160, 1072-82.
- [85] Wolf, J.A., Stys, P.K., Lusardi, T., Meaney, D., Smith, D.H. 2001. Traumatic axonal injury induces calcium influx modulated by tetrodotoxin-sensitive sodium channels. *J. Neurosci.* 21, 1923-30.
- [86] Yifrach, O., MacKinnon, R. 2002. Energetics of pore opening in a voltage-gated K(+) channel. *Cell.* 111, 231-9.
- [87] Zhang, Y., Gao, F., Popov, V.L, Wen, J.W., Hamill, O.P. 2000. Mechanically gated channel activity in cytoskeleton-deficient plasma membrane blebs and vesicles from *Xenopus* oocytes. *J. Physiol.* 523, 117-30.

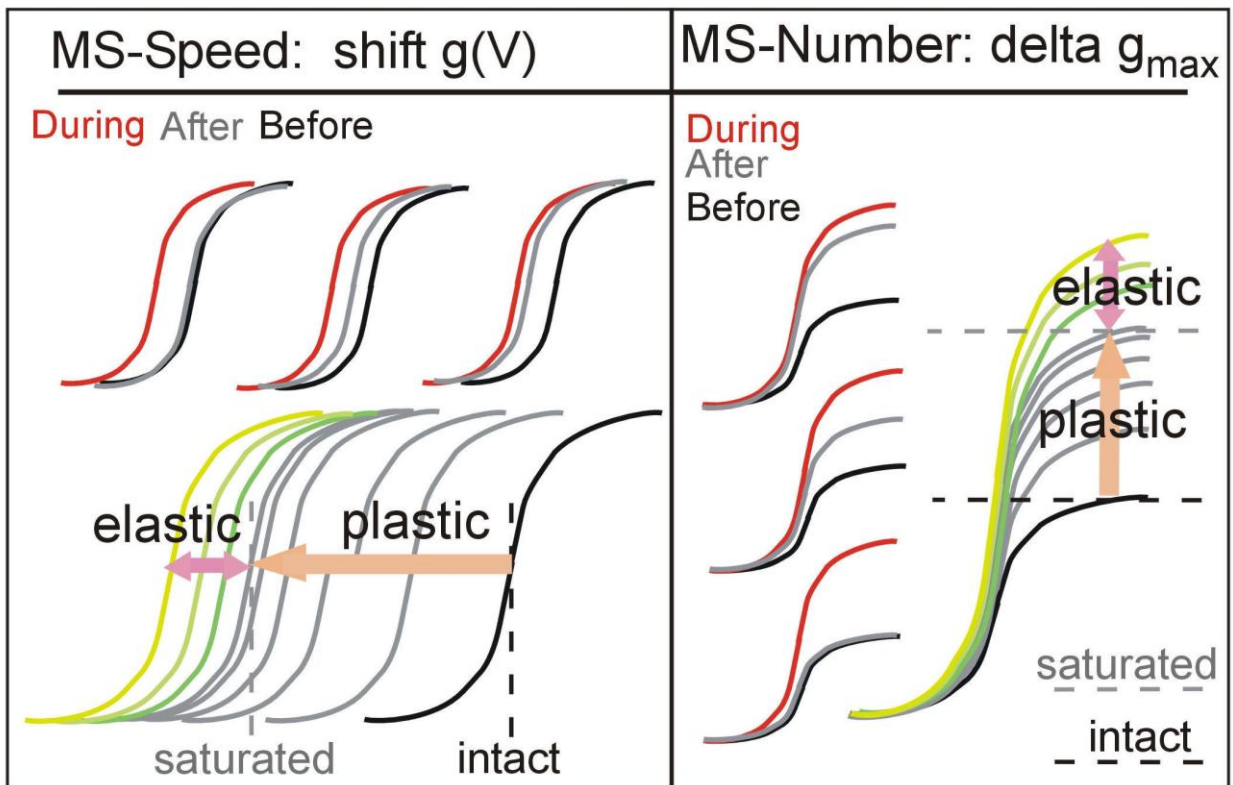


Figure 1 VCC activation and membrane stretch: MS-Speed and MS-Number responses. MS-Speed: shifts along the V_m -axis. MS-Number: a change in the apparent g_{max} . For stretch at a given intensity, $g(V)$ change can be reversible, partially reversible, or irreversible (before (black), during (red) and after stretch (grey)). In response to progressively increasing stretch intensity, $g(V)$ curves for VGCs in an intact membrane go through a range of plastic (irreversible) change which saturates at some point, after which stretch-intensity dependent reversible changes can be recorded without interference from concurrent irreversible change.

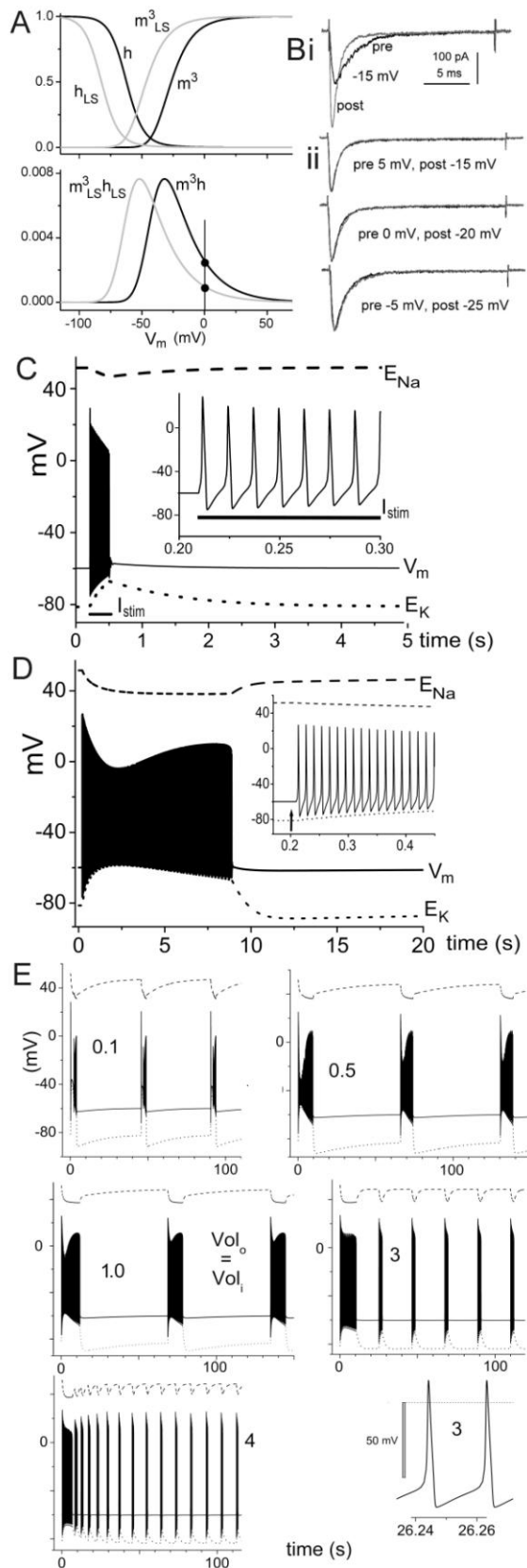


Figure 2

Nav-CLS injury and ectopic excitation.

A. Hodgkin-Huxley $m^3(V)$ and $h(V)$ plots for control conditions and with 20 mV hyperpolarizing (left) shifts; below, their steady-state products (window conductances). **B.** As explained in the text, i) irreversible response of recombinant Nav1.6 current to stretch, and ii) illustration of a 20 mV coupled left-shift. **C, D, E.** Computational results for a mildly traumatized axon, as described in the text. Expanded time resolution is provided in 3 instances to show action potential shapes. In **E**, the Nav-CLS injury (2 mV, all Nav channels) is the same in every case, with the only difference in the simulations being the different volume ratios $Vol_o:Vol_i$, as indicated by the numbers 0.1, 0.5, 1.0, 3 and 4.

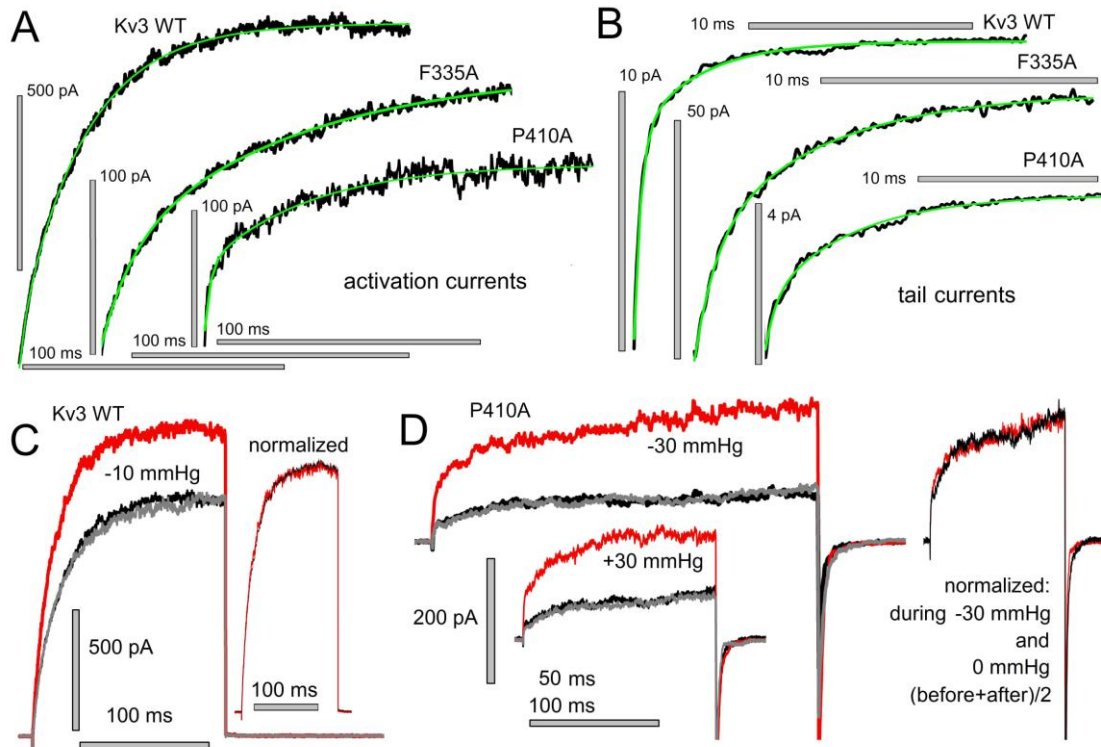


Figure 3 Kv3 channel kinetics without and with stretch: two open states and MS-Number responses. **A, B** Typical activation and tail current traces for Shaw Kv3 WT, F335A and P410A channels with overlaid fits (green) to sums of two exponentials. **C, D** For WT and P410A, traces before, during, after stretch (black, red, grey as per $g(V)$ relations of Fig 1) and at right for each, the average of before+after traces amplitude-normalized to the during-stretch trace. The complete overlap signifies that there has been no effect on kinetics, what changes with stretch is the number of channels participating; the Kv3 response to stretch appears to be comparable to the facilitating effect of pre-pulse depolarizations on cardiac L-type VGCa channels {13} where increased efficacy of coupling between sensor charge movement and pore opening is responsible.

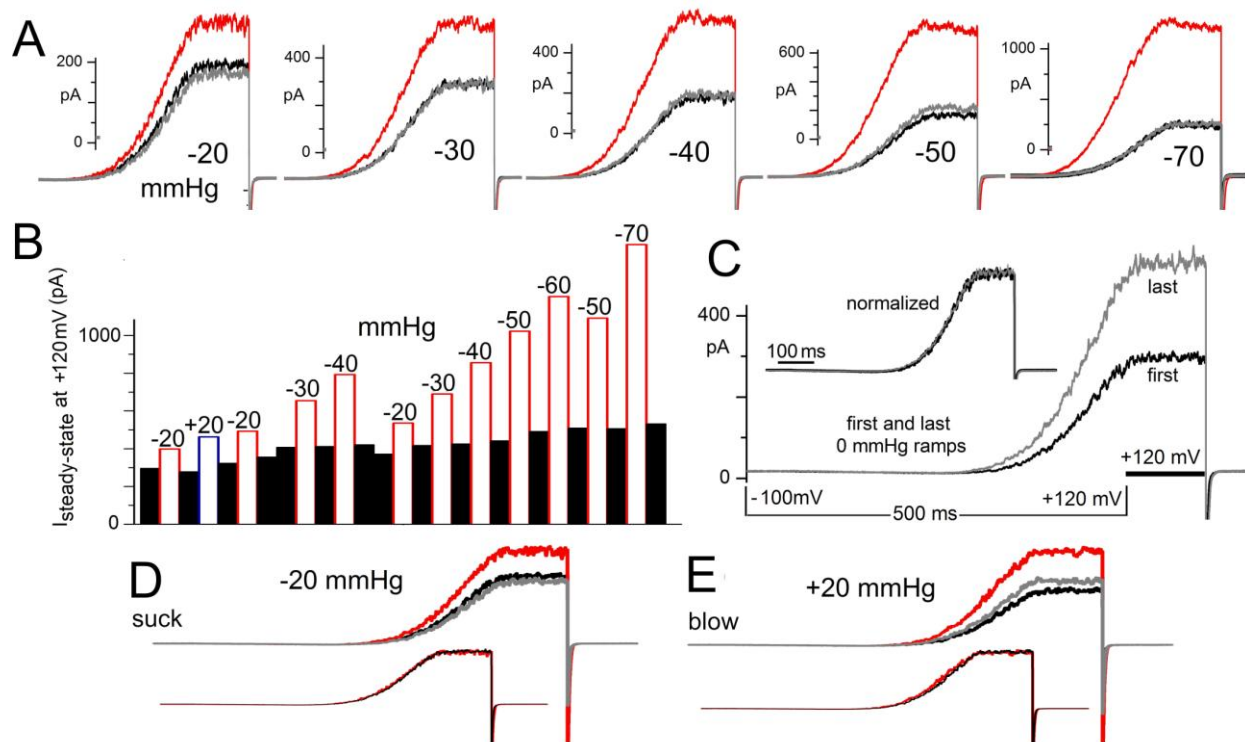


Figure 4 MS-Number behavior in Shaw Kv3 F335A using ramp-then-hold clamp. **A**, A series of before/during/after stretch traces with stretch applied by pipette aspiration (suction) at the intensity shown (mmHg). The voltage protocol: from $V_{hold} = -100$ mV, a 500 ms ramp to -120 mV and after 120 ms there, back to V_{hold} . (panel C labels these). Note that the I_K plateaus do *not* represent a g_{max} condition. They provide steady-state I_K at $+120$ mV (i.e. the y-axis in **B**). Note different current scales. Also note that by ~ -40 mmHg and beyond, stretch-modulated I_K exceeds depolarization-induced I_K . **B**, histogram summarizing the “stretch-dose” response experiment from which these traces are taken, with black=0 mmHg controls. In **C**, the first and last 0 mmHg traces are plotted then normalized (procedure as in Fig 3), and in **D**, **E** the full traces for -20 mmHg (first time) and $+20$ mmHg are plotted then normalized, illustrating MS-Number behavior as seen for ramp-then-hold currents and illustrating that blowing into the pipette is the equivalent of applying suction, as expected when increased bilayer tension is the modulating factor.

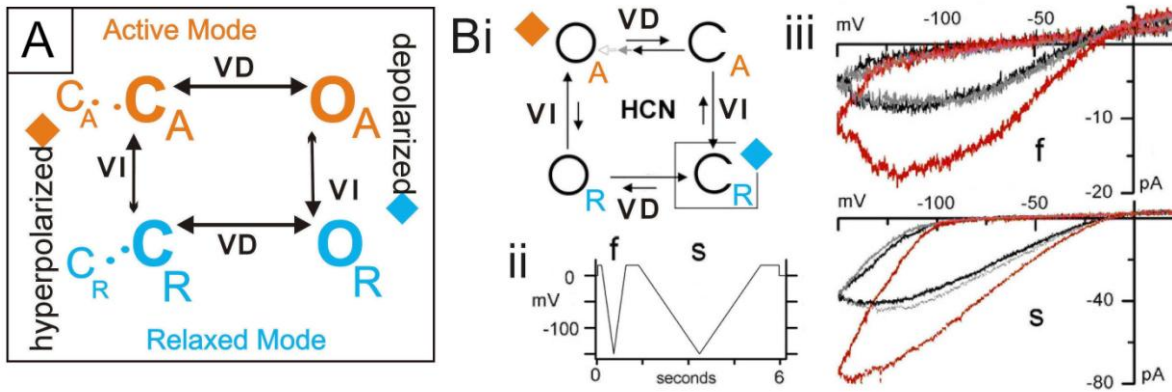


Figure 5 Mode-switch and MS modulation of VGCs. A, simplified scheme for Kv3 channels in closed/open (C,O) active/relaxed (A,R) mode states connected by voltage-dependent (VD) and voltage-independent (VI) transitions (the latter being the mode-switch transitions). In Kv3, VD transitions (and thus gating current motions) must occur between closed states indicated on the left of the diagram, but those transitions are not rate-limiting for pore opening. At least one must be a MS transition that augments the fraction of channels “ready-to-open-upon-depolarization”. This scheme is directly analogous to the mode-switch scheme used for HCN2 channels, {41}; it is redrawn in **Bi** with the naming and color conventions of **A**. In both schemes, prolonged hyperpolarization causes channels to populate states near the orange diamond while prolonged depolarization causes channels to populate near the blue diamond. Both are also analogous to a simplified mode-switch scheme for Nav channels {52}. **Bii**, **iii** illustrate the sawtooth ramp protocol (it includes first a fast, **f**, then a slower, **s**, voltage sawtooth) used to elicit the characteristic mode-switch-induced hysteresis of HCN2 cation currents elicited before, during, after stretch (modified from {41}).